

Synthesis and Structure Refinement of [Co–Al₄–X] LDHs (X = NO₃[−] and SO₄^{2−}) from Nordstrandite

Kavitha Venkataraman, Shivanna Marappa, and Grace S. Thomas*

Cite This: *ACS Omega* 2023, 8, 4782–4789

Read Online

ACCESS |



Metrics & More

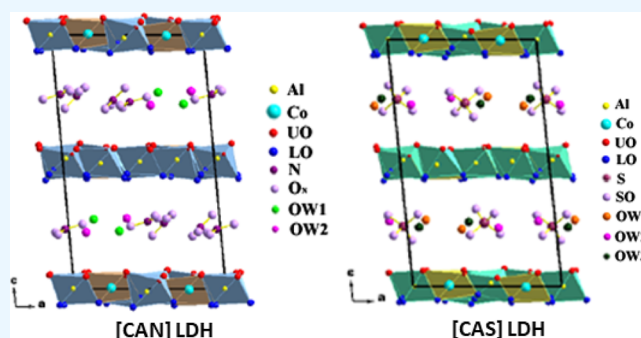


Article Recommendations



Supporting Information

ABSTRACT: [M–Al₄–X] LDHs (M = divalent metal and X = anion) are a class of aluminum-rich layered double hydroxides synthesized from both the gibbsite and bayerite polymorphs of Al(OH)₃. Henceforth, “g” and “b” are used to indicate gibbsite and bayerite. Despite the differences in the stacking arrangement of the hydroxyl layers in the precursor polymorphs, [M–Al₄–X] LDHs whether synthesized from gibbsite or bayerite were seen to be structurally the same. In this work, we report the first ever synthesis of [M–Al₄–X] LDHs (M = Zn, Ni, and Co and X = NO₃[−] and SO₄^{2−}) from nordstrandite, which is yet another polymorph of Al(OH)₃. Hereafter, “n” represents the nordstrandite precursor. We report that n-[M–Al₄–X] LDHs do not differ structurally from those prepared from gibbsite and bayerite. We also report the structural refinement of n-[Co–Al₄–X] LDHs, where X = NO₃[−] and SO₄^{2−}. This work is also significant as it gives for the very first time the refined structure of a [Co–Al₄–NO₃] LDH, though there are earlier reports on the synthesis of this LDH from both gibbsite and bayerite. The NO₃[−] ion in the interlayer makes an angle of ~48° with the plane of the metal hydroxide layer, and its symmetry reduces from D_{3h} to C_{2v}. Similarly, the change in the symmetry of the SO₄^{2−} ion in the interlayer is from T_d to C_{3v}.



INTRODUCTION

The polymorphs of aluminum hydroxide are obtained by stacking aluminum hydroxide layers one above the other using different stacking vectors. Each layer consists of a close packing of hydroxyl ions with two-third of the octahedral sites occupied by Al³⁺ ions and the other one-third being vacant, represented as [Al₂□(OH)₆] (□: cation vacancy). Imbibition of Li⁺ ions into the vacant sites introduces a positive charge on the layers to compensate which anions and water molecules occupy the interlayer region.¹ This structure is represented as [LiAl₂(OH)₆] [A^{n−}]_{1/n}·xH₂O (A^{n−} = Cl[−], Br[−], CO₃^{2−}, NO₃[−], SO₄^{2−}, and ClO₄[−]). This class of LDHs are the [Li–Al] LDHs.^{2–9} Instead of the monovalent Li⁺ if divalent metal ions M(II) (M = Zn, Ni, and Co) are introduced into the cation vacancies, by virtue of the difference in charge of the imbibed cations, only half of the octahedral vacancies will be occupied. A different class of LDHs is produced with layer composition [M_{0.5}□_{0.5}Al₂(OH)₆]⁺.^{10–12} The general formula of these LDHs is [M(II)Al₄(OH)₁₂](A^{n−})_{2/n}·yH₂O, henceforth referred to as [M–Al₄–X]. This class of LDHs have been synthesized from both gibbsite and bayerite, but there is no report on their synthesis from nordstrandite. Britto and Kamath have proposed a dissolution and reprecipitation mechanism for their formation.¹³ Hereinafter, we use g- to indicate the gibbsite precursor, b- to indicate the bayerite precursor, and n- to indicate the nordstrandite precursor.

The mineral equivalent of [M–Al₄–X] is nickel alumite [NiAl₄(OH)₁₂]SO₄·3H₂O. Uvarova et al. have refined this structure as monoclinic belonging to the space group P12₁/n.¹⁴

Fogg and co-workers first reported the synthesis of g-[M–Al₄–X] (M = Zn, Cu, Ni, and Co and X = NO₃[−]).¹⁰ Chitrakar et al. carried out anion-exchange studies of g-[Mg–Al₄–Cl] with Br[−], H₂PO₄[−], CO₃^{2−}, NO₃[−], BrO₃[−], and SO₄^{2−}.¹⁵ William and co-workers have explored the intercalation of organic carbonates and sulfonates in g-[M–Al₄–NO₃] (M = Zn, Cu, Ni, and Co) and orientation of anions with respect to the metal hydroxide layers.¹² William and O’Hare have refined the structure of g-[Zn–Al₄–NO₃] in the P12₁/c space group.¹⁶ The same group has synthesized a poorly ordered [Ni–Al₄–SO₄] from gibbsite but were unsuccessful in synthesizing [Co–Al₄–SO₄].¹² Rees et al. report g-[M–Al₄–Cl], where M = Co and Ni.¹⁷ Pachayappan and co-workers have refined the structure of g-[Ni–Al₄–NO₃] to a P12₁/n₁ space group.¹⁸ They observe a monoclinic to orthorhombic transformation of g-[Zn–Al₄–NO₃] at 160 °C without much change in the d-

Received: October 27, 2022

Accepted: January 13, 2023

Published: January 24, 2023



spacing.¹⁸ Szabados *et al.* in a recent work report the synthesis of [Cu–Al₄–X] LDHs (X = NO₃[−] and ClO₄[−]) starting from gibbsite.¹⁹

Britto and Kamath refined the structures of b-[Zn–Al₄–X] (X = SO₄^{2−} and NO₃[−]) with a P12₁/n₁ space group.¹³ They also report a high chromate sorption capacity for b-[Zn–Al₄–NO₃].²⁰ Jensen *et al.* report the optimum conditions for the synthesis of phase pure b-[Zn–Al₄–SO₄].²¹ Pushparaj *et al.* synthesized [Zn–Al₄–SO₄] and refined the structure using the P12₁/n space group.²² Anderson *et al.* in a 2021 work reports the synthesis and thermal studies of b-[M–Al₄–SO₄] (M = Zn, Cu, Ni, and Co).²³ Though they report the Rietveld refinement of these LDHs, their reported χ^2 value ranging from 1800 to 18,700 seem unrealistic according to Brain H Toby.²⁴

All reported refinements of [M–Al₄–X] synthesized from both gibbsite and bayerite show these LDHs to have a monoclinic structure.

In this work, we have attempted the synthesis of [M–Al₄–X], where M = Zn, Ni, and Co and X = NO₃[−] and SO₄^{2−}, from nordstrandite to address the following questions.

- Will the use of nordstrandite as a precursor yield [M–Al₄–X] LDHs which are structurally different from those of gibbsite and bayerite?
- Can we obtain from nordstrandite [M–Al₄–X] LDHs which have not been synthesized from gibbsite and bayerite?

RESULTS AND DISCUSSION

Part I. This part deals with [M–Al₄–X], where M = Zn and Ni and X = NO₃[−] and SO₄^{2−} from nordstrandite to address the question (i) asked earlier.

All the prepared LDHs except [Ni–Al₄–SO₄] were ordered as can be seen by their powder X-ray diffraction (PXRD) patterns (Figures S1 and S2). Though [Ni–Al₄–SO₄] is poorly ordered, its cell parameters calculated from the PXRD pattern are a good match with the reported values of the mineral nickel alumite.¹⁴ The PXRD patterns of [Zn–Al₄–X], X = NO₃[−] and SO₄^{2−}, were compared with the reported patterns of the corresponding LDHs from both gibbsite and bayerite (Table S1) and a good match was found.^{13,18,20}

Williams *et al.* have reported the synthesis of a poorly ordered g-[Ni–Al₄–SO₄].¹² [Ni–Al₄–SO₄] obtained by us from nordstrandite is also poorly ordered (Figure S2). We were not successful in optimizing the conditions to obtain crystalline [Ni–Al₄–SO₄] LDH.

Part II. This part deals with the synthesis of [Co–Al₄–NO₃] and [Co–Al₄–SO₄] LDHs from nordstrandite and henceforth represented as [CAN] and [CAS] LDHs, respectively.

There is no report on the synthesis of [CAS] from gibbsite. However, while writing this paper, Anderson and group reported on the synthesis of [CAS] from bayerite. Though [CAN] is reported to crystallize in a two-layer monoclinic structure, the Rietveld refinement was not performed.¹³ In this work, we report the refinement of [CAN] and [CAS] LDHs.

[CAN] LDH. The PXRD pattern of [CAN] LDH consists of two basal reflections at 2θ 10.27 and 20.69° (Figure S3). The PXRD pattern was indexed to a two-layer cell of monoclinic symmetry, and the refined cell parameters obtained are $a = 10.2917 \text{ \AA}$, $b = 8.9200 \text{ \AA}$, $c = 17.2558 \text{ \AA}$, and $\beta = 95.51^\circ$ (Table 1). The FTIR spectra confirmed the intercalation of the NO₃[−] ion. A free nitrate ion always exists in the D_{3h} symmetry

Table 1. Observed 2θ Values [°] and the Corresponding hkl Indices of [CAN] LDH

[CAN] LDH	
$a = 10.2917 \text{ \AA}$, $b = 8.9200 \text{ \AA}$, $c = 17.2558 \text{ \AA}$, $\alpha = \gamma = 90.0^\circ$, $\beta = 95.51^\circ$	
FM value = 3.922, De Wolff's Mn value = 4.920	
2θ [deg]	hkl
10.28	002
18.54	201
19.30	−202
20.69	004
22.43	022
24.30	−213
26.42	213
27.86	−222
29.00	−312
30.53	031
31.63	−106
32.86	016
33.96	033
35.49	133
39.09	126
40.50	−421
41.13	−422
42.83	404
45.07	501
50.20	−523
55.80	054
58.89	351
62.46	060
63.47	−451
66.57	064
68.83	065
71.40	455
73.95	732
76.27	−556
78.12	−653
80.39	−466

in the ionic solution, which would show two active modes of vibrations. In the case of monodentate and bidentate nitrate ions, the symmetry reduces to either C_{2v} or C_s, and the number of vibrational modes increase. The reduced symmetry of the NO₃[−] ion is indicated by the splitting of the ν_3 vibration mode at 1401 and 1364 cm^{−1} and the other bands at 962, 848, 716, and 590 cm^{−1} (Figure 1). All the six vibrational frequencies suggest that the symmetry of the NO₃[−] ion reduces from D_{3h} to C_{2v}.^{18,25–29}

The Al³⁺ and Co²⁺ content obtained from energy-dispersive X-ray analysis (EDAX) gave an Al/Co ratio of ~3.5 pointing to the presence of excess cobalt in the synthesized sample (Figure S4). The thermogravimetric analysis (TGA) gives information about the mass loss with an increase in temperature. In typical LDH materials, mass loss below 100 °C corresponds to the adsorbed water molecules, 100–200 °C corresponds to an intercalated water molecule, and above 200 °C till 450–500 °C, the mass loss corresponds to the dehydroxylation (metal hydroxide layer collapse), and further heating to higher temperature leads to de-anation and convert them to spinels.^{30,31} TGA shows an overall mass loss of 43.71% at 950 °C (Figure 2). The residue is mapped to the formula 0.6CoO + 1.025Al₂O₃. The first step mass loss of 8% corresponds to ~1.3 moles. Hence, the approximate formula

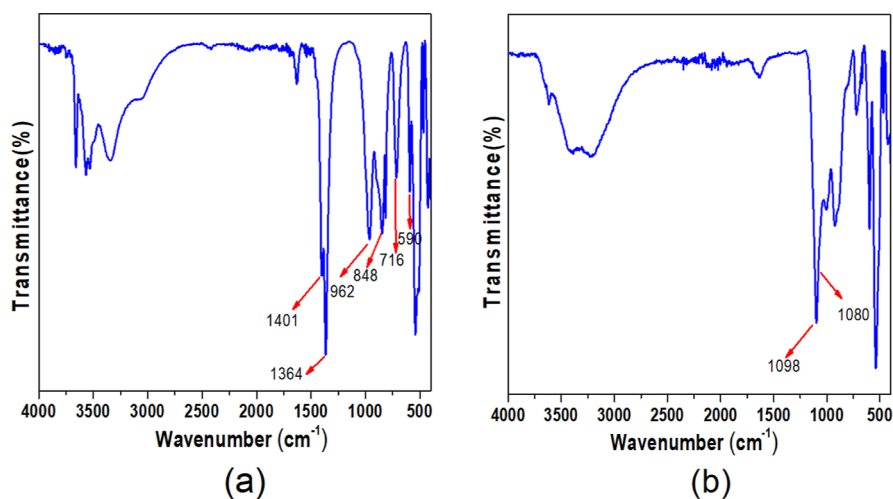


Figure 1. IR spectra of (a) [CAN] LDH. (b) [CAS] LDH.

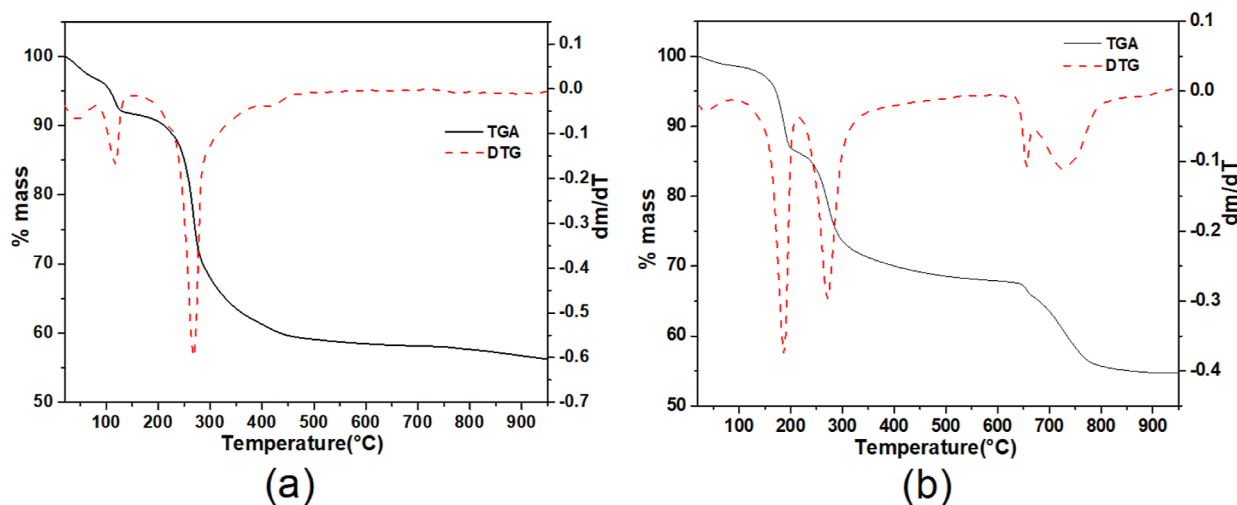


Figure 2. TGA of (a) [CAN] LDH. (b) [CAS] LDH.

of the LDH can be written as $[\text{Co}_{0.6}\text{Al}_{2.05}(\text{OH})_6](\text{NO}_3)_{0.55} \cdot 1.3\text{H}_2\text{O}$ (Table 2).

Table 2. Compositional Analysis of [CAN] and [CAS] LDHs

sample	Al/Co ratio	A ^{III} /Co ratio	overall mass loss from TGA (%)	approximate composition of the sample
[CAN] LDH	3.5	0.92	43.71	$[\text{Co}_{0.6}\text{Al}_{2.05}(\text{OH})_6](\text{NO}_3)_{0.55} \cdot 1.3\text{H}_2\text{O}$
[CAS] LDH	4.44	1.06	45.23	$[\text{Co}_{0.54}\text{Al}_{2.4}(\text{OH})_6](\text{SO}_4)_{0.57} \cdot 2.7\text{H}_2\text{O}$

[CAS] LDH. The first two basal reflections of [CAS] LDH appear at 2θ 10.34 and 20.79° in the PXRD pattern (Figure S5). The pattern was indexed to a two-layer monoclinic cell, and the refined lattice parameters are $a = 10.3364$ Å, $b = 8.9179$ Å, $c = 17.1953$ Å, and $\beta = 95.65^\circ$ (Table 3). The intercalation of the SO_4^{2-} ion is confirmed by FTIR spectra. In solution, the SO_4^{2-} ion exists in a tetrahedral symmetry and would show two active modes of vibration (ν_3 and ν_4). In the monodentate SO_4^{2-} ion, the symmetry reduces to C_{3v} , the number of vibrational modes increase (ν_1 , ν_2 , ν_3 , and ν_4), and also ν_3 and ν_4 split into two modes. In the case of a bidentate

SO_4^{2-} ion, the symmetry reduces to C_{2v} , the number of vibrational modes increase (ν_1 , ν_2 , ν_3 , and ν_4), and also ν_3 and ν_4 split into three modes. A sharp band at 1098 cm^{-1} and a shoulder at 1080 cm^{-1} corresponding to SO_4^{2-} are observed. The other vibrational modes are shrouded by lattice vibrations (Figure 1).^{13,32,33}

The ratio of the metal ions Al/Co in the sample is 4.44 as obtained from EDAX (Figure S6). TGA shows an overall mass loss of 45.23%. The mass of the residue is attributed to $0.54\text{CoO} + 1.2\text{Al}_2\text{O}_3$, and the first step mass loss of 12.67% corresponds to ~ 2.7 moles of H_2O (Figure 2). The approximate formula is written as $[\text{Co}_{0.54}\text{Al}_{2.4}(\text{OH})_6] \cdot (\text{SO}_4)_{0.57} \cdot 2.7\text{H}_2\text{O}$ (Table 2). This formula indicates a higher water content compared to other reported LDHs of this class.^{11–23}

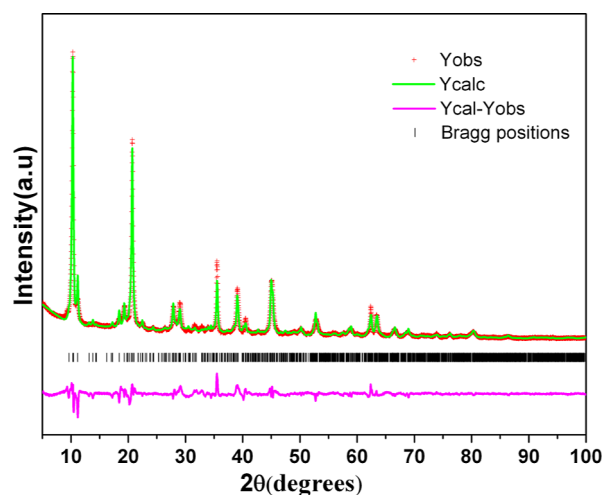
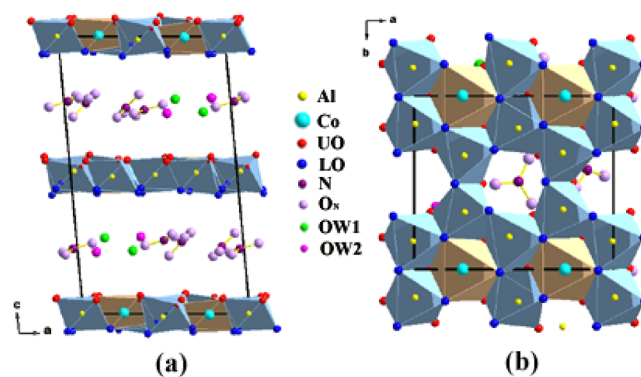
Structure Refinement of [CAN] LDH. The cell parameters and space group obtained from indexing were validated by performing a Le Bail fit in the space group $P12_1/n1$ in code FOX.³⁴ All the Bragg reflections were produced with satisfactory R values ($R_{\text{wp}} = 3.45$ and $R_p = 3.74$). The partial structure model of the metal hydroxide layer borrowed from the reported structure of the [Ni–Al₄–NO₃] LDH was then given as the input in code FOX. A Monte Carlo approach was used to identify the position of anions and water molecules

Table 3. Observed 2θ Values [$^{\circ}$] and the Corresponding hkl Indices of [CAS] LDH

[CAS] LDH	
$a = 10.3364 \text{ \AA}, b = 8.9179 \text{ \AA}, c = 17.1953 \text{ \AA}, \alpha = \gamma = 90.0^{\circ}, \beta = 95.65^{\circ}$	
FM value = 5.3630, De Wolff's Mn value = 4.0766	
2θ [deg]	hkl
10.33	002
11.17	011
13.14	-110
13.80	-111
14.46	111
16.21	-112
17.30	112
18.44	013
19.22	-202
20.79	004
21.10	113
22.48	022
23.90	-114
24.23	-213
25.38	-204
26.63	-221
27.92	015
29.11	222
32.74	-224
34.02	-206
35.54	133
37.52	402
38.33	-413
39.17	126
40.60	-135
41.41	-140
43.03	142
45.27	510
48.97	-522
50.22	244
53.08	245
58.91	-535
59.95	-353
62.38	-543
63.52	062
66.62	064
69.12	-640
73.94	-462
76.25	172
80.38	735

after introducing them into the interlayer region. They were allowed to freely translate and rotate in the interlayer. Refinement showed two water molecules with the anions and water molecules midway between the layers. The nitrate ions make an angle of $\sim 48^{\circ}$ with the metal hydroxide layer. At last, the coordinates of the metal hydroxide layer were refined, which yielded unacceptable Co–O bond lengths and O–Co–O bond angles; hence, coordinates of the metal hydroxide layer were retained as such. At this stage, the R_{wp} and R_p values were 8.94 and 9.66 with a good match between the observed and computed patterns. This structure was transferred to the FULLPROF suite to complete the refinement in reciprocal space.³⁵ The Rietveld fit of the PXRD pattern of the [CAN] LDH and refined structure (CCDC no. 2164867) are given in Figures 3 and 4. The refined parameters, atomic coordinates,

refined bond distances, and angles are given in Tables 4, S2, and S4.

**Figure 3.** Rietveld fit of the PXRD pattern of the [CAN] LDH.**Figure 4.** Refined structure of the [CAN] LDH viewed (a) along the b -crystallographic axis. (b) Along the c -crystallographic axis.**Table 4. Results of Rietveld Refinement of the [CAN] LDH and [CAS] LDH**

	[CAN] LDH	[CAS] LDH
formula unit	$[\text{CoAl}_4(\text{OH})_{12}](\text{NO}_3) \cdot 2\text{H}_2\text{O}$	$[\text{CoAl}_4(\text{OH})_{12}](\text{SO}_4) \cdot 4\text{H}_2\text{O}$
crystal system	monoclinic	monoclinic
space group	$P12_1/n1$	$P12_1/n1$
a (\AA)	10.3159(12)	10.3172(6)
b (\AA)	8.9171(9)	8.9210(5)
c (\AA)	17.2184(8)	17.1861(5)
α (deg)	90	90
β (deg)	95.21(8)	96.02(4)
γ (deg)	90	90
volume (\AA^3)	1577.30(3)	1573.09(13)
parameters refined	16	17
R_{wp}	5.86	5.73
R_p	4.01	4.20
R_{exp}	1.38	1.55
R_F	5.81	6.26
χ^2	18.1	13.8

Structure of the [CAS] LDH. A Le Bail fit in the space group $P12_1/n1$ in code FOX matched all Bragg reflections in the PXRD pattern ($R_{wp} = 3.0$ and $R_p = 3.31$). The input file in code FOX for the partial structure model of the metal hydroxide layers was the reported structure of the $[\text{Ni}-\text{Al}_4-\text{NO}_3]$ LDH.¹⁸ After introducing the anions and water molecules in the interlayer region, a Monte Carlo approach was used to locate their positions by allowing them to move freely in the interlayer. The position and occupancy of the interlayer species were refined. Anions and water molecules took positions equidistant to the layers. A good match between the observed and computed patterns was obtained ($R_{wp} = 8.86$ and $R_p = 9.63$). The refinement carried out in FOX was in direct space. To complete the refinement in reciprocal space, the structure model was taken to the FULLPROF suite.³⁵ The final R -values obtained were 5.73 and 4.20. In the refined structure, one of the four S–O bonds (S–O14) is 1.4979 Å, while the other three S–O bonds have become shorter (1.43–1.44 Å). This causes a reduction in the symmetry of the sulfate ion from T_d to C_{3v} . Hydrogen bonding between sulfate oxygens and layers is stronger than hydrogen bonding to the water molecules (Table S5). The Rietveld fit of the [CAS] LDH and the refined structure are given in Figures 5 and 6, and the results of Rietveld refinement are given in Tables 4, S3, and S5.

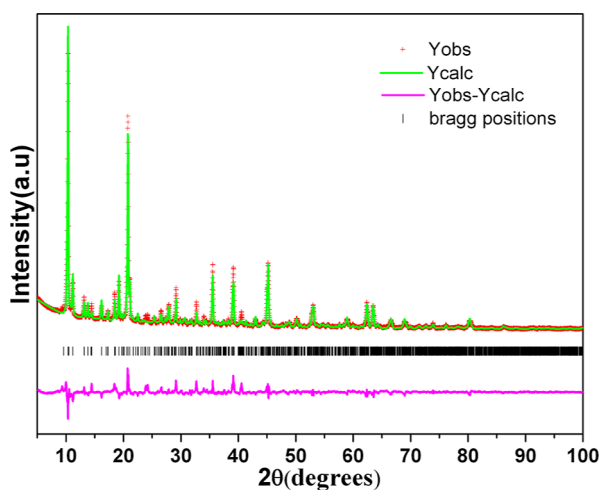


Figure 5. Rietveld fit of the PXRD pattern of the [CAS] LDH.

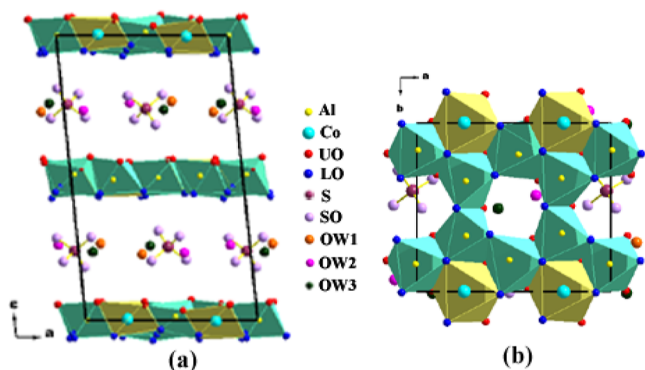


Figure 6. Refined structure of the [CAS] LDH viewed (a) along the b -crystallographic axis and (b) along the c -crystallographic axis.

Dehydration–Rehydration Studies on the [CAN] LDH. The in situ high-temperature phase at 170 °C was

indexed to a cell of orthorhombic symmetry (Figure 7 and Table 5). The PXRD pattern matched the reported structure

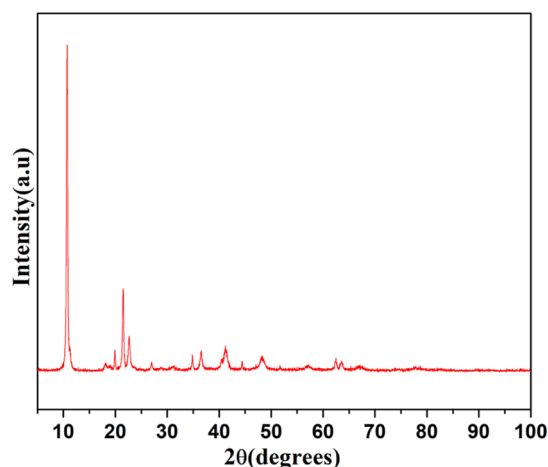


Figure 7. PXRD pattern of [CAN] (DH) LDH.

Table 5. Observed 2θ Values [°] and the Corresponding hkl Indices of the [CAN] (DH) LDH

[CAN] (DH) LDH	
$a = 5.0925 \text{ \AA}, b = 8.9585 \text{ \AA}, c = 16.5218 \text{ \AA}, \alpha = \beta = \gamma = 90^\circ$	
FM value = 4.9298, De Wolff's Mn value = 7.3255	
2θ [deg]	hkl
10.7	002
11.23	011
18.18	101
19.83	020
21.48	004
22.58	022
27.00	005
28.80	015
31.14	123
34.87	130
36.52	132
40.66	041
41.27	134
44.54	141
48.28	232
57.24	243
62.45	061
63.51	250
66.60	064
67.61	2010

of the g - $[\text{Zn}-\text{Al}_4-\text{NO}_3]$ dehydrate (Table 6).¹⁸ We conclude that both g and n - $[\text{M}-\text{Al}_4-\text{X}]$ LDHs yield an orthorhombic polytype on dehydration.

Gibbsite, bayerite, and nordstrandite differ in the stacking arrangement of their aluminum hydroxide layers. Gibbsite is a two-layer polytype with a layer stacking arrangement $\bar{P}\bar{P}\bar{P}$, where \bar{P} is the mirror image of P. Both bayerite and nordstrandite have a PPP layer stacking with a slight translation of the layers in nordstrandite. Gibbsite has a two-layer monoclinic structure, whereas bayerite has a single-layer monoclinic structure. Nordstrandite alone is triclinic with a one-layer structure. Despite the differences in the crystal

Table 6. Cell Parameters and 2θ Positions of Basal Reflections of High-Temperature Phases of $[M-Al_4]$ LDHs

sample	cell parameters	2θ positions of 002, 004 reflections
$g-[Zn-Al_4-NO_3]^{15}$ (DH)	$a = 5.16 \text{ \AA}$, $b = 8.97 \text{ \AA}$, $c = 16.56 \text{ \AA}$	10.7, 21.5
[CAN] (DH)	$a = 5.09 \text{ \AA}$, $b = 8.96 \text{ \AA}$, $c = 16.52 \text{ \AA}$	10.7, 21.5

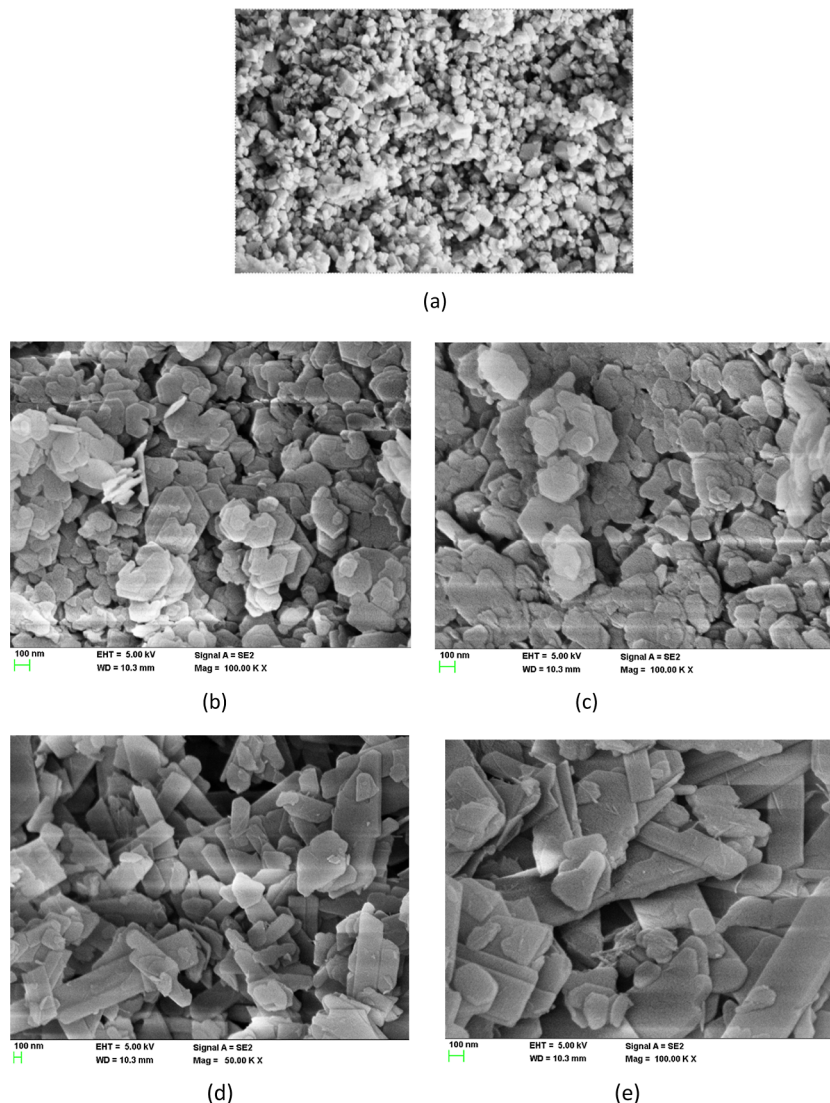
symmetry of the precursor, all $[M-Al_4-X]$ LDHs irrespective of the precursor have similar PXRD patterns. While this has already been reported in the case for $[M-Al_4]$ LDHs from gibbsite and bayerite, in this work, we report that nordstrandite too does not give a new series of $[M-Al_4-X]$ LDHs. This confirms the mechanism of formation of these LDHs to be dissolution and reprecipitation as proposed by Britto and Kamath.¹³

Refinement of [CAN] and [CAS] LDHs place them in a $P12_1/n_1$ space group. Dehydration of the [CAN] LDH caused a change in polytype from monoclinic to orthorhombic. These results are in keeping with earlier reports on $g-[Zn-Al_4-NO_3]$.¹⁸ We conclude that the dehydration behavior of this

class of LDHs is the same irrespective of the precursor used for the as-prepared LDH. This is in contrast to the behavior of the $[Li-Al-X]$ LDHs.^{2-7,36}

William et al. have reported that attempts to synthesize ordered [CAN] and [CAS] LDHs from gibbsite proved unsuccessful.¹² Britto and Kamath report that they were unable to synthesize the [CAS] LDH from bayerite.¹³ However, Anderson et al. have successfully prepared CAS from bayerite. However, the synthesis reported by Anderson involves a 14 day hydrothermal synthesis at 120°C . The successful synthesis of both $[Co-Al_4-NO_3]$ and $[Co-Al_4-SO_4]$ from nordstrandite point toward the metastable nature of nordstrandite. In an earlier work, Venkataraman and Pachayappan have reported that the C_1 symmetry of the nordstrandite interlayer renders it metastable.³⁷ We propose that it is this metastable nature of nordstrandite that allows its facile conversion to $[M-Al_4-X]$ LDHs.

A difference in morphology between the precursor nordstrandite (triclinic) and LDH (monoclinic) is evident in their SEM micrographs (Figure 8). The SEM image of nordstrandite (Figure 8a) is strikingly similar to that of triclinic $AlPO_4$.³⁸ The SEM micrograph of [CAS] (Figure 8d,e) reveals

**Figure 8.** SEM micrograph images of (a) nordstrandite. (b) and (c) [CAN] LDH. (d) and (e) [CAS] LDH.

the typical monoclinic morphology (rod like morphology). Though the morphology of [CAN] (Figure 8b,c) looks different from [CAS], there are regions where they appear the same.

CONCLUSIONS

Imbibition of divalent metal ions into the cation vacancies of nordstrandite yield LDHs, which are similar to those formed from the other polymorphs of $\text{Al}(\text{OH})_3$, namely, gibbsite and bayerite. This confirms a dissolution reprecipitation mechanism of formation reported in earlier work. The successful synthesis of phase pure [CAS] and [CAN] LDHs from nordstrandite implies that it is the metastable nature of nordstrandite that favors its facile conversion into an LDH. This opens up possibilities for the use of nordstrandite as a precursor for the synthesis of a variety of LDHs. The dehydrated phases of these LDHs are similar irrespective of the precursor used to prepare the LDHs.

EXPERIMENTAL SECTION

Synthesis. Nordstrandite was synthesized by Taichi's procedure (Figure S7).³⁹ $\text{Al}(\text{OH})_3$ gel was precipitated at pH 8 by the addition of 25% NH_3 to a 0.25 M AlCl_3 solution at a rate of 5 mL min^{-1} at 25°C . The gel was thoroughly washed with deionized water and aged in 8% ethylene diamine solution at 40°C for 40 h. The nordstrandite obtained was washed with water and dried. To prepare the LDHs, 0.5 g of nordstrandite was soaked in 10 mL of a supersaturated solutions of nitrate and sulfate salts of Zn, Ni, and Co. The solutions were treated hydrothermally for 24 h in a Teflon-lined autoclave of capacity 80 mL at the following temperatures: 150°C for $\text{Co}(\text{NO}_3)_2$, CoSO_4 , $\text{Zn}(\text{NO}_3)_2$, ZnSO_4 and 180°C for $\text{Ni}(\text{NO}_3)_2$ and NiSO_4 . The product obtained after hydrothermal treatment was washed with Type II water (specific resistance $15 \text{ M}\Omega \text{ cm}$, Millipore Academic water purification system) and dried in a hot air oven at 60°C .^{13,18}

Characterization. All the samples were characterized through PXRD using a Bruker D8 ADVANCE diffractometer (Cu-K α radiation, Ni filter, $\lambda = 1.5418 \text{ \AA}$) operating in reflection geometry (40 kV and 30 mA). An Anton Paar CHC plus Humidity Chamber was used as an attachment for the dehydration–rehydration studies of the $[\text{Co}-\text{Al}_4-\text{NO}_3]$ LDH. A Rigaku Smart Lab diffractometer (Cu-K α radiation, K β filter, $\lambda = 1.5418 \text{ \AA}$, 40 kV, 30 mA) was used for the slow scan of both $[\text{Co}-\text{Al}_4-\text{SO}_4]$ and $[\text{Co}-\text{Al}_4-\text{NO}_3]$ LDHs. Code APPLEMAN, a part of PROZKI suite of programs, was used to index the PXRD patterns and obtain the cell parameters.⁴⁰ TGA was performed to estimate the amount of intercalated water over a temperature range of $30\text{--}900^\circ\text{C}$ at a heating rate of 3°C min^{-1} in a N_2 atmosphere using a Mettler Toledo TG (SDTA) model 851e system driven by STARe 7.01 software. The Al^{3+} , Co^{2+} , and sulfate contents in the samples were estimated through EDAX. The nitrate content was estimated by ion chromatography (Metrohm model 861 advanced compact ion chromatograph fitted to a Metrosep SUP5 150 column). Intercalation of anions was confirmed by IR spectra using a Bruker Alpha-P IR spectrometer (diamond attenuated total reflectance cell, $400\text{--}4000 \text{ cm}^{-1}$, 4 cm^{-1} resolution).

ASSOCIATED CONTENT

Supporting Information

The Supporting Information is available free of charge at <https://pubs.acs.org/doi/10.1021/acsomega.2c06914>.

PXRD patterns of $[\text{Ni}-\text{Al}_4-\text{NO}_3]$, $[\text{Zn}-\text{Al}_4-\text{SO}_4]$, and $[\text{Zn}-\text{Al}_4-\text{NO}_3]$ from the nordstrandite precursor; PXRD pattern of $[\text{Ni}-\text{Al}_4-\text{SO}_4]$; PXRD pattern of the [CAN] LDH; EDAX of the [CAN] LDH; PXRD pattern of the [CAS] LDH; EDAX of the [CAS] LDH; PXRD pattern of nordstrandite; comparison of d-spacing of $[\text{M}-\text{Al}_4-\text{X}]$ LDHs; refined atomic coordinates of the [CAN] LDH; bond distances and bond angles of the [CAN] LDH; refined atomic coordinates of the [CAS] LDH; and bond distances and bond angles of the [CAS] LDH (PDF)

Co- Al_4 - NO_3 (CIF)

Co- Al_4 - SO_4 (CIF)

checkCIF/PLATON report for CAN (PDF)

checkCIF/PLATON report for CAS (PDF)

Accession Codes

CCDC 2164867 ([CAN] LDH) and CCDC 2164868 ([CAS] LDH) contain the supplementary crystallographic data for this paper and are obtained free of charge via www.ccdc.cam.ac.uk/data_request/cif

AUTHOR INFORMATION

Corresponding Author

Grace S. Thomas – Department of Chemistry, Jyoti Nivas College, Bangalore 560 095, India; orcid.org/0000-0002-1712-4320; Email: gracesaraht@gmail.com

Authors

Kavitha Venkataraman – Department of Chemistry, Jyoti Nivas College, Bangalore 560 095, India

Shivanna Marappa – Department of Chemistry, REVA University, Bangalore 560 064, India; orcid.org/0000-0003-1814-9930

Complete contact information is available at: <https://pubs.acs.org/10.1021/acsomega.2c06914>

Notes

The authors declare no competing financial interest.

ACKNOWLEDGMENTS

K.V. thanks P. V. Kamath and Jyoti Nivas College. S.M. thanks REVA University and management for the seed money support (RU:EST:CH:2022/16, dated 28/02/2022).

REFERENCES

- (1) Komarneni, S.; Kozai, N.; Roy, R. Novel Function for Anionic Clays: Selective Transition Metal Cation Uptake by Diadochy. *J. Mater. Chem.* **1998**, *8*, 1329–1331.
- (2) Britto, S.; Kamath, P. V. Polyttypism in the Lithium-Aluminum Layered Double Hydroxides: The $[\text{LiAl}_2(\text{OH})_6]^+$ Layer as a Structural Synthon. *Inorg. Chem.* **2011**, *50*, 5619–5627.
- (3) Britto, S.; Kamath, P. V. Structure of Bayerite-Based Lithium - Aluminum Layered Double Hydroxides (LDHs) : Observation of Monoclinic Symmetry. *Inorg. Chem.* **2009**, *48*, 11646–11654.
- (4) Nagendran, S.; Periyasamy, G.; Kamath, P. V. Structure Models for the Hydrated and Dehydrated Nitrate-Intercalated Layered Double Hydroxide of Li and Al. *Dalton Trans.* **2016**, *45*, 18324–18332.

- (5) Nagendran, S.; Periyasamy, G.; Kamath, P. V. Hydration-Induced Interpolytype Transformations in the Bayerite-Derived Nitrate-Intercalated Layered Double Hydroxide of Li and Al. *J. Solid State Chem.* **2018**, *266*, 226–232.
- (6) Pachayappan, L.; Kamath, P. V. Effect of Hydration on Polytypism and Disorder in the Sulfate-Intercalated Layered Double Hydroxides of Li and Al. *Clays Clay Miner.* **2019**, *67*, 154–162.
- (7) Pachayappan, L.; Kamath, P. V. Reversible Hydration of the Perchlorate-Intercalated Layered Double Hydroxides of Li and Al: Structure Models for the Dehydrated Phases. *Bull. Mater. Sci.* **2020**, *43*, 141.
- (8) Besserguenev, A. V.; Fogg, A. M.; Francis, R. J.; Price, S. J.; O'Hare, D.; Isupov, V. P.; Tolochko, B. P. Synthesis and Structure of the Gibbsite Intercalation Compounds $[\text{LiAl}_2(\text{OH})_6]\text{X}$ $\{\text{X} = \text{Cl}, \text{Br}, \text{NO}_3\}$ and $[\text{LiAl}_2(\text{OH})_6]\text{Cl}\cdot\text{H}_2\text{O}$ Using Synchrotron X-Ray and Neutron Powder Diffraction. *Chem. Mater.* **1997**, *9*, 241–247.
- (9) Fogg, A. M.; O'Hare, D. Study of the Intercalation of Lithium Salt in Gibbsite Using Time-Resolved in Situ x-Ray Diffraction. *Chem. Mater.* **1999**, *11*, 1771–1775.
- (10) Fogg, A. M.; Williams, G. R.; Chester, R.; O'Hare, D. A Novel Family of Layered Double Hydroxides— $[\text{MAl}_4(\text{OH})_{12}](\text{NO}_3)_2\cdot x\text{H}_2\text{O}$ ($\text{M} = \text{Co}, \text{Ni}, \text{Cu}, \text{Zn}$). *J. Mater. Chem.* **2004**, *14*, 2369–2371.
- (11) Williams, G. R.; Dunbar, T. G.; Beer, A. J.; Fogg, A. M.; O'Hare, D. Intercalation Chemistry of the Novel Layered Double Hydroxides $[\text{MAl}_4(\text{OH})_{12}](\text{NO}_3)_2\cdot y\text{H}_2\text{O}$ ($\text{M} = \text{Zn}, \text{Cu}, \text{Ni}$ and Co). 2: Selective Intercalation Chemistry. *J. Mater. Chem.* **2006**, *16*, 1231–1237.
- (12) Williams, G. R.; Moorhouse, S. J.; Prior, T. J.; Fogg, A. M.; Rees, N. H.; O'Hare, D. New Insights into the Intercalation Chemistry of $\text{Al}(\text{OH})_3$. *Dalton Trans.* **2011**, *44*, 6012–6022.
- (13) Britto, S.; Kamath, P. V. Polytypism, Disorder, and Anion Exchange Properties of Divalent Ion (Zn, Co) Containing Bayerite-Derived Layered Double Hydroxides. *Inorg. Chem.* **2010**, *49*, 11370–11377.
- (14) Uvarova, Y. U. A.; Sokolova, E. L.; Hawthorne, F. R. C.; Karpenko, V. V.; Agakhanov, A. A.; Pautov, L. A. The Crystal Chemistry of the “Nickelalumite”-Group Minerals. *Can. Mineral.* **2005**, *43*, 1511–1519.
- (15) Chitrakar, R.; Makita, Y.; Sonoda, A.; Hirotsu, T. Synthesis of a Novel Layered Double Hydroxides $[\text{MgAl}_4(\text{OH})_{12}](\text{Cl})_2\cdot 2.4\text{H}_2\text{O}$ and Its Anion-Exchange Properties. *J. Hazard. Mater.* **2011**, *185*, 1435–1439.
- (16) Williams, G. R.; O'Hare, D. Towards Understanding, Control and Application of Layered Double Hydroxide Chemistry. *J. Mater. Chem.* **2006**, *16*, 3065–3074.
- (17) Rees, J. R.; Burden, C. S.; Fogg, A. M. New Layered Double Hydroxides by Prepared by the Intercalation of Gibbsite. *J. Solid State Chem.* **2015**, *224*, 36–39.
- (18) Pachayappan, L.; Nagendran, S.; Kamath, P. V. Polytypism in Alumite-like Layered Double Hydroxides of M (Zn^{2+} , Ni^{2+}) and Al: A Structural Transformation from Monoclinic to Orthorhombic Symmetry. *Cryst. Growth Des.* **2020**, *20*, 3264–3271.
- (19) Szabados, M.; Ádám, A. A.; Kása, Z.; Baán, K.; Mucsi, R.; Sági, A.; Kónya, Z.; Kukovec, Á.; Sipos, P. M(II)Al₄ Type Layered Double Hydroxides—Preparation Using Mechanochemical Route, Structural Characterization and Catalytic Application. *Materials* **2021**, *14* (). DOI: 10.3390/ma14174880
- (20) Britto, S.; Kamath, P. V. Synthesis, Structure Refinement and Chromate Sorption Characteristics of an Al-Rich Bayerite-Based Layered Double Hydroxide. *J. Solid State Chem.* **2014**, *215*, 206–210.
- (21) Jensen, N. D.; Duong, N. T.; Bolanz, R.; Nishiyama, Y.; Rasmussen, C. A.; Gottlicher, J.; Steininger, R.; Prevot, V.; Nielsen, U. G. Synthesis and Structural Characterization of a Pure ZnAl₄(OH)₁₂(SO₄)₂·2.6H₂O Layered Double Hydroxide. *Inorg. Chem.* **2019**, *58*, 6114–6122.
- (22) Pushparaj, S. S. C.; Jensen, N. D.; Forano, C.; Rees, G. J.; Prevot, V.; Hanna, J. V.; Ravnsbæk, D. B.; Bjerring, M.; Nielsen, U. G. Structural Investigation of Zn(II) Insertion in Bayerite, an Aluminum Hydroxide. *Inorg. Chem.* **2016**, *55*, 9306–9315.
- (23) Andersen, A. B. A.; Henriksen, C.; Wang, Q.; Ravnsbæk, D. B.; Hansen, L. P.; Nielsen, U. G. Synthesis and Thermal Degradation of $\text{MAl}_4(\text{OH})_{12}\text{SO}_4\cdot 3\text{H}_2\text{O}$ with $\text{M} = \text{Co}^{2+}$, Ni^{2+} , Cu^{2+} , and Zn^{2+} . *Inorg. Chem.* **2021**, *60*, 16700–16712.
- (24) Toby, B. H. R factors in Rietveld analysis: How good is good enough? *Powder Diffr.* **2006**, *21*, 67–70.
- (25) Arizaga, G. G. C.; Mangrich, A. S.; da Costa Gardolinski, J. E. F.; Wypych, F. Chemical Modification of Zinc Hydroxide Nitrate and Zn-Al-Layered Double Hydroxide with Dicarboxylic Acids. *J. Colloid Interface Sci.* **2008**, *320*, 168–176.
- (26) Wang, S.-L.; Wang, P.-C. In Situ XRD and ATR-FTIR Study on the Molecular Orientation of Interlayer Nitrate in Mg/Al-Layered Double Hydroxides in Water. *Colloids Surf., A* **2007**, *292*, 131–138.
- (27) Chen, M.; Zhu, R.; Lu, X.; Zhu, J.; He, H. Influences of Cation Ratio, Anion Type, and Water Content on Polytypism of Layered Double Hydroxides. *Inorg. Chem.* **2018**, *57*, 7299–7313.
- (28) Yadav, D. K.; Uma, S.; Nagarajan, R. Microwave-assisted synthesis of ternary Li-M-Al LDHs ($\text{M} = \text{Mg}, \text{Co}, \text{Ni}, \text{Cu}, \text{Zn}$, and Cd) and examining their use in phenol oxidation. *Appl. Clay Sci.* **2022**, *228*, 106655.
- (29) Marappa, S.; Radha, S.; Kamath, P. V. Nitrate-Intercalated Layered Double Hydroxides - Structure Model, Order, and Disorder. *Eur. J. Inorg. Chem.* **2013**, *2013*, 2122–2128.
- (30) Marappa, S.; Kamath, P. V. Interaction of Pristine Hydrotalcite-like Layered Double Hydroxides with CO₂: A Thermogravimetric Study. *Bull. Mater. Sci.* **2015**, *38*, 1783–1790.
- (31) Sotiles, A. R.; Gomez, N. A. G.; Wypych, F. Thermogravimetric Analysis of Layered Double Hydroxides Intercalated with Sulfate and Alkaline Cations $[\text{M}_6\text{Al}_3(\text{OH})_{18}][\text{A}+(\text{SO}_4)_2] \cdot 12\text{H}_2\text{O}$ ($\text{M}_2 = \text{Mn}, \text{Mg}, \text{Zn}$; $\text{A} = \text{Li}, \text{Na}, \text{K}$). *J. Therm. Anal. Calorim.* **2020**, *140*, 1715–1723.
- (32) Lane, M. D. Mid-Infrared Emission Spectroscopy of Sulfate and Sulfate-Bearing Minerals. *Am. Mineral.* **2007**, *92*, 1–18.
- (33) Secco, E. A. Spectroscopic properties of SO₄ (and OH) in different molecular and crystalline environments. I. Infrared spectra of $\text{Cu}_4(\text{OH})_6\text{SO}_4$, $\text{Cu}_4(\text{OH})_4\text{OSO}_4$, and $\text{Cu}_3(\text{OH})_4\text{SO}_4$. *Can. J. Chem.* **1988**, *66*, 329–336.
- (34) Favre-Nicolin, V.; Černý, R. FOX, “Free Objects for Crystallography”: A Modular Approach to Ab Initio Structure Determination from Powder Diffraction. *J. Appl. Crystallogr.* **2002**, *35*, 734–743.
- (35) Rodriguez-Carvajal, J. Fullprof: A Program for Rietveld Refinement and Pattern Matching Analysis. *Abstract of the Satellite Meeting on Powder Diffraction of the XV Congress of the IUCr: Toulouse, France, 1990; Vol. 127.*
- (36) Venkataraman, K.; Thomas, G. S. Dehydration-Rehydration Studies on Polytypes of Chloride and Nitrate Layered Double Hydroxides of Nordstrandite and Bayerite: A Comparative Study. *ACS Omega* **2022**, *7*, 5393–5400.
- (37) Venkataraman, K.; Pachayappan, L. Synthesis of Nordstrandite and Nordstrandite-Derived Layered Double Hydroxides of Li and Al: A Comparative Study with the Bayerite Counterpart. *Z. Anorg. Allg. Chem.* **2020**, *646*, 1916–1921.
- (38) Wu, J.; Zhao, H.; Li, N.; Luo, Q.; He, C.; Guan, N.; Xiang, S. Fluorine-Free Crystallization of Triclinic $\text{AlPO}_4\cdot 3\text{H}_2\text{O}$. *CrystEngComm* **2012**, *14*, 8671–8676.
- (39) Taichi, S. Preparation of Aluminum Hydride. *J. Jpn. Inst. Light Met.* **1988**, *38*, 731–739.
- (40) Lasocha, W.; Lewinski, K. PROSZKI – a system of programs for powder diffraction data analysis. *J. Appl. Crystallogr.* **1994**, *27*, 437–438.